

RESEARCH ARTICLE

Effects of fluid and norepinephrine resuscitation in a sheep model of endotoxin shock and acute kidney injury

Gonzalo Ferrara,¹ Vanina Siham Kanoore Edul,¹ Juan Francisco Caminos Eguillor,¹ María Guillermina Buscetti,¹ Héctor Saúl Canales,¹ Bernardo Lattanzio,¹ Luis Gatti,¹ Can Ince,² and Arnaldo Dubin¹

¹Facultad de Ciencias Médicas, Universidad Nacional de La Plata, Cátedra de Farmacología Aplicada, La Plata, Argentina; and ²Department of Intensive Care, Erasmus MC, University Medical Center Rotterdam, Rotterdam, The Netherlands

Submitted 15 March 2019; accepted in final form 25 June 2019

Ferrara G, Kanoore Edul VS, Caminos Eguillor JF, Buscetti MG, Canales HS, Lattanzio B, Gatti L, Ince C, Dubin A. Effects of fluid and norepinephrine resuscitation in a sheep model of endotoxin shock and acute kidney injury. *J Appl Physiol* 127: 788–797, 2019. First published July 11, 2019; doi:10.1152/jappphysiol.00172.2019.—The pathophysiology of renal failure in septic shock is complex. Although microvascular dysfunction has been proposed as a mechanism, there are controversial findings about the characteristics of microvascular redistribution and the effects of resuscitation. Our hypothesis was that the normalization of systemic hemodynamics with fluids and norepinephrine fails to improve acute kidney injury. To test this hypothesis, we assessed systemic and renal hemodynamics and oxygen metabolism in 24 anesthetized and mechanically ventilated sheep. Renal cortical microcirculation was evaluated by SDF-video microscopy. Shock ($n = 12$) was induced by intravenous administration of endotoxin. After 60 min of shock, 30 mL/kg of saline solution was infused and norepinephrine was titrated to reach a mean blood pressure of 70 mmHg for 2 h. These animals were compared with a sham group ($n = 12$). After endotoxin administration, mean blood pressure, cardiac index, and systemic O₂ transport and consumption decreased ($P < 0.05$ for all). Resuscitation improved these variables. Endotoxin shock also reduced renal blood flow and O₂ transport and consumption (205[157–293] vs. 131 [99–185], 28.4 [19.0–38.2] vs. 15.8[13.5–23.2], and 5.4[4.0–8.8] vs. 3.7[3.3–4.5] mL·min⁻¹·100 g⁻¹, respectively); cortical perfused capillary density (23.8[23.5–25.9] vs. 17.5[15.1–19.0] mm/mm²); and creatinine clearance (62.4[39.2–99.4] vs. 10.7[4.4–23.5] mL/min). After 2 h of resuscitation, these variables did not improve (174[91–186], 20.5 [10.8–22.7], and 3.8[1.9–4.8] mL·min⁻¹·100 g⁻¹, 19.9[18.6–22.1] mm/mm², and 5.9[1.0–11.9] mL/min). In conclusion, endotoxin shock induced severe renal failure associated with decreased renal flow, O₂ transport and consumption, and cortical microcirculation. Normalization of systemic hemodynamics with fluids and norepinephrine failed to improve renal perfusion, oxygenation, and function.

NEW & NOTEWORTHY This experimental model of endotoxin shock induced severe renal failure, which was associated with abnormalities in renal regional blood flow, microcirculation, and oxygenation. Derangements included the compromise of peritubular microvascular perfusion. Improvements in systemic hemodynamics through fluids and norepinephrine were unable to correct these abnormalities.

blood flow; creatinine clearance; endotoxin shock; microcirculation; renal failure

Address for reprint requests and other correspondence: A. Dubin, Facultad de Ciencias Médicas, Universidad Nacional de La Plata, Cátedra de Farmacología Aplicada, La Plata, Argentina (e-mail: arnaldodubin@gmail.com).

INTRODUCTION

Sepsis is a leading cause of death in critically ill patients. It frequently produces acute kidney injury (AKI), which additionally increases mortality (2, 12). Septic AKI has been related to ischemia resulting from reductions in renal blood flow (RBF) (30). Experimental research, however, showed that RBF was preserved in most of the AKI models (21). Hence, different investigators have proposed the dysfunction of microcirculation as the underlying mechanism of renal failure (9, 26).

There are controversial reports about the characteristics of microvascular dysfunction in septic AKI. A growing body of evidence points to redistribution of blood flow away from the renal medulla, with preservation of cortical perfusion and oxygenation (3, 19). In contrast, other studies found alterations in cortical perfusion (22, 34).

Most of the evaluations that described unchanged cortical perfusion were based on laser Doppler flowmetry (3, 19). This technique gives global measurements of tissue perfusion that can overlook microcirculatory heterogeneity (33). In addition, reports of cortical video microscopic alterations have been focused only on specific variables (13, 22). Therefore, a comprehensive assessment of renal cortical microcirculation, including density, perfusion, and heterogeneity characteristics, and its relationship with regional and systemic hemodynamics, is lacking.

Our goal was to evaluate the behavior of cortical peritubular microcirculation in a model of endotoxin shock and resuscitation and its relationship with global renal perfusion, oxygenation, and function. We also aimed at comparing microcirculatory dysfunction among renal cortical, intestinal villi, and sublingual vascular beds. Our main hypothesis was that resuscitation with a fixed fluid challenge and norepinephrine targeted to a mean arterial pressure (MAP) of 70 mmHg, in accordance with the Surviving Sepsis Campaign guidelines, fails to improve renal perfusion and function (28).

MATERIALS AND METHODS

The local Research Committee approved this study [Protocol number P01-05-2016]. The care of animals was in accordance with the National Institutes of Health.

Anesthesia and ventilation. Twenty-four sheep (24 ± 5 kg, means \pm SD) were anesthetized with 30 mg/kg of pentobarbital sodium, intubated, and mechanically ventilated with a Servo Ventilator 900C (Siemens-Elementa, Solna, Sweden) with a tidal volume

of 10 mL/kg, a fraction of inspired oxygen ($F_{I_{O_2}}$) of 0.21 and a positive end-expiratory pressure of 6 cmH₂O. The initial respiratory rate was set to keep the arterial P_{CO_2} between 35 and 40 mmHg. This respiratory setting was maintained during the rest of the experiment. Neuromuscular blockade was performed with pancuronium bromide (0.06 mg/kg). Additional pentobarbital boluses (1 mg/kg) were administered hourly and when clinical signs of inadequate depth of anesthesia were evident. Analgesia was provided by fentanyl as a bolus of 2 μ g/kg, followed by 1 μ g·kg⁻¹·h⁻¹. These drugs were administered intravenously.

Surgical preparation. A schematic drawing of the surgical preparation is shown in Fig. 1. A 7.5-French Swan-Ganz Standard Thermodilution Pulmonary Artery Catheter (Edwards Life Sciences, Irvine, CA) was inserted in the right external jugular vein to obtain mixed venous samples. Catheters were placed in the descending aorta via the left femoral artery to measure blood pressure and obtain blood samples, and in the inferior vena cava to administer fluids and drugs.

A midline laparotomy was performed, followed by a gastrostomy to drain gastric contents, and a splenectomy to avoid spleen contraction during shock. Perivascular ultrasonic flow probes were placed around the superior mesenteric artery and the left renal artery, to measure intestinal blood flow (IBF) and RBF. Catheters were introduced in the left renal and mesenteric vein to draw blood samples and to measure venous pressure. Catheters were also positioned in the abdomen for intra-abdominal pressure measurement and into the bladder to monitor urinary output. To allow renal cortical videomicroscopy, the left kidney was gently decapsulated and 5-cm incision was performed in the left flank of the abdominal wall. A tonometer was inserted through a small ileotomy to measure intramucosal PCO_2 . A 10- to 15-cm segment of the ileum was mobilized, placed outside the abdomen, and opened 2 cm on the antimesenteric border to allow

examination of mucosal microcirculation. The exteriorized intestinal segment was covered and moistened, and the temperature was preserved by an external heating device. Finally, after complete hemostasis, the midline abdominal wall incision was closed, except for a short segment for externalization of the ileal loop.

Measurements and derived calculations. Systemic O_2 consumption ($\dot{V}O_2$) was measured by analysis of expired gases (MedGraphics CPX Ultima, Medical Graphics, St. Paul, MN) and adjusted to body weight.

Arterial, mixed venous, renal venous, and mesenteric venous PO_2 , PCO_2 , pH, Hb, and O_2 saturation were measured with a blood-gas analyzer and a co-oximeter calibrated for sheep blood (ABL 5 and OSM 3, Radiometer, Copenhagen, Denmark). Oxygen-derived variables were calculated by standard formulas.

Since the thermodilution method overestimates low cardiac output, the cardiac index (CI) was calculated as $\dot{V}O_2$ divided by arterial-mixed venous O_2 content difference ($C_{a-mv}O_2$). Systemic and pulmonary vascular resistance were calculated as MAP minus central venous pressure divided by cardiac output, and mean minus wedge pulmonary pressure divided by cardiac output, respectively. Systemic O_2 transport (DO_2) was calculated as CI multiplied by arterial O_2 content (Ca_{O_2}). The systemic O_2 extraction ratio (O_2ER) was calculated as $C_{a-mv}O_2$ divided by Ca_{O_2} .

IBF and RBF were measured by an ultrasonic flowmeter (One Channel Perivascular Flowmeter, Transonics Systems, Ithaca, NY) and normalized to the organ weight. Intestinal and left renal vascular resistances were calculated as MAP minus mesenteric or left renal venous pressure divided by IBF or RBF.

Intestinal and renal DO_2 and $\dot{V}O_2$ were calculated as the product of the respective flow index multiplied by either Ca_{O_2} or arteriovenous oxygen content difference. Intestinal and renal O_2ER were calculated

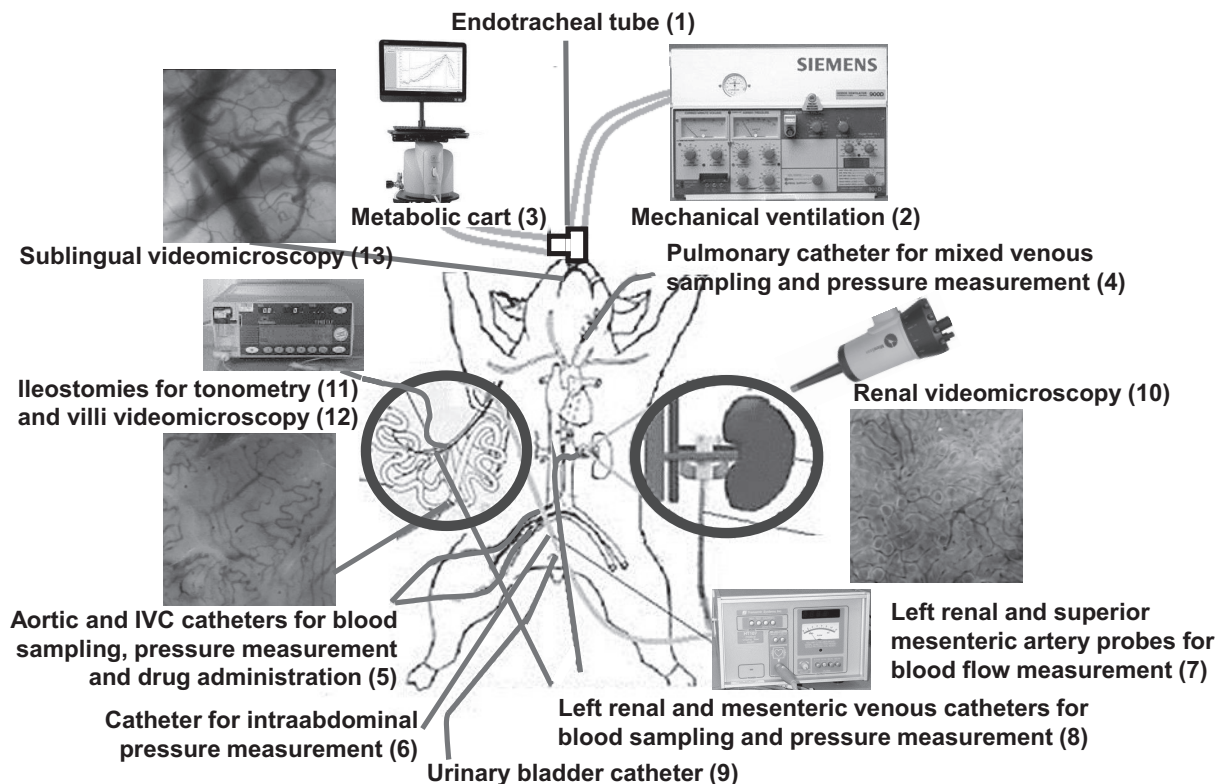


Fig. 1. Schematic drawing of the surgical preparation. Endotracheal tube (1) for mechanical ventilation (2) and analysis of expired gases; pulmonary catheter for mixed venous sampling and pressure measurement (4); aortic and inferior vena cava (IVC) catheters for blood sampling, pressure measurement, and administration of fluids and drugs (5); catheter for measurement of intra-abdominal pressure (6); left renal and superior mesenteric artery probes for blood flow measurement (7); left renal and mesenteric venous catheters for blood sampling and pressure measurement (8); urinary bladder catheter (9); renal decapsulation for videomicroscopy (10); ileostomies for tissue capnography (11) and villi videomicroscopy (12); and sublingual videomicroscopy (13).

as the respective arteriovenous oxygen content difference divided by CaO_2 .

Intramucosal PCO_2 was measured by air tonometry (Tonometrics Catheter and Tonocap, Datex-Ohmeda, Helsinki, Finland). Then, we calculated mucosal-arterial PCO_2 difference.

Arterial lactate was measured with a point-of-care analyzer (Stat Profile Critical Care Xpress, Nova Biomedical, Waltham, MA).

Creatinine clearance was calculated as the urinary creatinine multiplied by the urine output in 60 min divided by the plasma creatinine.

Microvideoscopic measurements and analysis. The microcirculatory network was evaluated in renal cortex, intestinal mucosa, and sublingual mucosa by means of a SDF imaging device (Microscan, MicroVision Medical, Amsterdam, The Netherlands) (8). Different precautions were taken and steps followed to obtain images of adequate quality and to ensure satisfactory reproducibility. After gentle removal of secretions by isotonic saline-drenched gauze, steady images of at least 20 s were obtained while avoiding pressure artifacts with a portable computer and an analog-to-digital video converter (ADVC110, Canopus, San Jose, CA). The videos were recorded from three different areas. Video clips were stored as AVI files to allow computerized frame-by-frame image analysis.

Video image analysis was performed blindly by well-trained researchers. Adequate focus and contrast adjustment were verified, and images of poor quality were discarded. The entire sequence was used to describe the semiquantitative characteristics of the microvascular flow and, particularly, the presence of stopped or intermittent flow.

We used image-analysis software (Microscan analysis software AVA 3.2-MicroVision Medical) (7) to determine total vascular density (TVD). An analysis based on semiquantitative criteria that distinguished no flow (0), intermittent flow (1), sluggish flow (2), and continuous flow (3) was performed on individual vessels. The overall score, called MFI, is the average of the individual values (27). Quantitative red blood cell (RBC) velocity was determined using space-time diagrams (7). We also calculated the proportion of perfused vessels (PPV), the perfused vascular density (PVD) as TVD multiplied by PPV, and the heterogeneity flow index (HFI) as highest-lowest MFI divided by the mean MFI (35).

In sheep, most of sublingual vascular density ($97 \pm 1\%$) and all peritubular renal and intestinal villi vessels consist of small vessels (diameter $<25 \mu\text{m}$), so analysis was focused on this type of vessel, whereas the vessels of higher diameter were assessed only for ruling out compression artifacts.

Experimental procedure. Basal measurements were taken after a period of no less than 30 min after MAP, systemic $\dot{V}\text{O}_2$, and renal and intestinal flow became stable. Animals were then randomly assigned to endotoxin shock ($n = 12$) or sham ($n = 12$) groups. In the endotoxin shock group, shock was induced by intravenous injection of *Escherichia coli* lipopolysaccharide ($5 \mu\text{g}/\text{kg}$ followed by $2.5 \mu\text{g}\cdot\text{kg}^{-1}\cdot\text{h}^{-1}$ for 180 min). After 60 min of shock, 30 mL/kg of saline solution were infused and norepinephrine was titrated to reach a MAP of 70 mmHg. In the sham group, the same experimental preparation was carried out, and 0.9% NaCl was infused to maintain hemodynamic variables at basal values, without further interventions. Measurements were performed at baseline (0 min), after 60 min of endotoxin shock without resuscitation, and after 60 and 120 min of resuscitation. Blood temperature was kept constant throughout the study with a heating lamp.

At the end of the experiment, animals were euthanized with an additional dose of pentobarbital sodium and a KCl bolus. A catheter was inserted in superior mesenteric artery and India ink was instilled through it. Dyed intestinal segments were dissected, washed, and weighed. We also weighed the left kidney. Consequently, intestinal and renal flow, $\dot{V}\text{O}_2$, and DO_2 are expressed as indices of the organ weight.

Data analysis. Because of the small numbers of animals, nonparametric tests were used. Changes over time within each group were assessed with nonparametric analysis of variance for repeated mea-

surements (Friedman test) followed by a post hoc test (Dunn's multiple comparison test). Differences between groups at each time point were analyzed with a Mann-Whitney *U*-test. The renal $\dot{V}\text{O}_2/\text{DO}_2$ relationship was assessed with linear regression analysis. Data are expressed as median and interquartile range. A *P* value <0.05 was considered statistically significant.

RESULTS

Systemic effects. Endotoxin administration decreased MAP, CI, and systemic vascular resistance. $\dot{V}\text{O}_2$ and DO_2 fell, and O_2ER increased. Resuscitation normalized CI, $\dot{V}\text{O}_2$, and DO_2 . MAP increased until the target values but remained lower than in the sham group. Norepinephrine requirements were $3.2[2.5\text{--}5.0] \mu\text{g}\cdot\text{kg}^{-1}\cdot\text{min}^{-1}$. Endotoxin induced pulmonary hypertension. In the sham group, all variables remained unchanged. Hemodynamic changes are shown in Table 1, and changes in lactate and blood gases in Supplemental Table S1 (<https://doi.org/10.6084/m9.figshare.8115872>).

Renal effects. RBF and DO_2 decreased after endotoxin injection, transiently improved with resuscitation, and eventually fell. $\dot{V}\text{O}_2$ decreased after endotoxin administration and remained so during the rest of the experiment. O_2ER never increased and fell at 60 min of resuscitation. Vascular resistance decreased after 60 min of endotoxin shock and normalized with resuscitation (Table 1 and Fig. 2).

$\dot{V}\text{O}_2$ and DO_2 were strongly correlated in both groups (Fig. 3).

After 60 min of endotoxin shock, there were derangements in all the microcirculatory variables. Resuscitation only normalized RBC velocity (Fig. 4 and Supplemental Video S1 <https://doi.org/10.6084/m9.figshare.8115875.v1>).

Urinary output and creatinine clearance decreased during endotoxin shock and remained low during the resuscitation phase (Fig. 5).

Intestinal effects. Endotoxin shock diminished intestinal flow, DO_2 , and vascular resistance and augmented O_2ER . $\dot{V}\text{O}_2$ remained unchanged. Resuscitation normalized flow, DO_2 , and resistance, while O_2ER persisted elevated (Table 1).

Except for manifest and persistent increases in HFI, villi microcirculation only showed minor and transitory alterations (Fig. 6). Mucosal-arterial PCO_2 difference was higher in endotoxin shock than in the sham group (Fig. 7).

Sublingual effects. During shock, there were alterations in PPV, MFI, RBC velocity, and HFI. After resuscitation, only RBC velocity remained reduced compared with the sham group (Fig. 8).

DISCUSSION

In this experimental model of endotoxin shock, the main finding was the development of severe renal failure, which was associated with reductions in RBF, cortical microcirculation, and renal vascular resistance. Regardless of the improvement in systemic hemodynamics, kidney derangements were unresponsive to aggressive fluid and norepinephrine resuscitation. After 2-h of resuscitation, RBF and microvascular perfusion, renal $\dot{V}\text{O}_2$ and DO_2 , and creatinine clearance remained significantly disturbed.

Unlike other experimental studies that showed mild to moderate reductions in renal function (3, 19), our model was characterized by severe and persistent decrease in urine output

Table 1. Values of systemic, intestinal, and renal hemodynamic variables in sham and endotoxin shock groups

| | Basal | 60 Min | 120 Min | 180 Min |
|--|------------------|---------------------|--------------------|---------------------|
| Heart rate, beats/min | | | | |
| Sham | 157 [143–156] | 160 [146–174] | 176 [135–190] | 161 [150–181] |
| Endotoxin shock | 155 [125–172] | 122 [106–131]*† | 167 [156–200] | 165 [132–180] |
| Mean arterial pressure, mmHg | | | | |
| Sham | 80 [74–94] | 87 [78–99] | 93 [75–106] | 93 [74–106] |
| Endotoxin shock | 83 [71–98] | 34 [31–40]*† | 72 [70–74]† | 71 [70–73]† |
| Central venous pressure, mmHg | | | | |
| Sham | 2 [0–4] | 1 [0–4] | 2 [0–4] | 2 [0–4] |
| Endotoxin shock | 4 [2–6] | 3 [2–5] | 5 [1–9] | 7 [2–9]† |
| Mean pulmonary pressure, mmHg | | | | |
| Sham | 12 [12–16] | 14 [11–18] | 15 [12–21] | 14 [11–18] |
| Endotoxin shock | 14 [10–18] | 14 [13–17] | 21 [18–25]*† | 24 [21–25]*† |
| Pulmonary occlusion pressure, mmHg | | | | |
| Sham | 2 [1–3] | 3 [2–4] | 3 [1–4] | 3 [0–4] |
| Endotoxin shock | 2 [1–4] | 2 [1–3] | 3 [1–5] | 4 [2–5] |
| Mesenteric venous pressure, mmHg | | | | |
| Sham | 4 [2–6] | 5 [4–6] | 5 [4–7] | 5 [5–7] |
| Endotoxin shock | 5 [4–6] | 6 [4–9] | 7 [6–9]*† | 9 [7–10]*† |
| Renal venous pressure (mmHg) | | | | |
| Sham | 3 [1–4] | 2 [1–5] | 2 [1–4] | 2 [1–4] |
| Endotoxin shock | 3 [1–5] | 3 [1–6] | 5 [3–6] | 4 [2–6] |
| Intra-abdominal pressure, mmHg | | | | |
| Sham | 1 [0–1] | 1 [0–1] | 1 [0–2] | 1 [0–1] |
| Endotoxin shock | 1 [0–1] | 1 [0–1] | 1 [0–1] | 1 [0–2] |
| Cardiac index, mL·min ⁻¹ ·kg ⁻¹ | | | | |
| Sham | 144 [123–168] | 135 [125–192] | 144 [122–174] | 159 [120–210] |
| Endotoxin shock | 138 [110–161] | 90 [73–113]*† | 174 [110–244] | 161 [129–183] |
| Superior mesenteric artery flow, mL·min ⁻¹ ·100 g ⁻¹ | | | | |
| Sham | 44.0 [34.2–57.4] | 41.3 [33.1–60.3] | 46.0 [36.2–60.6] | 48.8 [43.7–69.4] |
| Endotoxin shock | 44.2 [29.1–67.7] | 26.2 [21.9–47.8]*† | 36.2 [24.9–52.0] | 40.7 [24.5–63.1] |
| Systemic vascular resistance, mmHg·L ⁻¹ ·min ⁻¹ | | | | |
| Sham | 25.1 [21.8–29.6] | 28.1 [24.2–33.9] | 32.4 [22.4–33.9] | 27.2 [22.6–34.8] |
| Endotoxin shock | 27.8 [17.8–40.2] | 18.6 [10.6–25.5]*† | 17.5 [14.5–29.7]*† | 19.6 [15.4–25.5]*† |
| Pulmonary vascular resistance, mmHg·L ⁻¹ ·min | | | | |
| Sham | 4.11 [3.37–5.08] | 4.29 [3.53–5.02] | 4.41 [3.35–5.98] | 4.19 [2.61–5.03] |
| Endotoxin shock | 4.43 [3.55–6.76] | 7.77 [6.00–10.17]*† | 6.29 [4.60–9.16] | 6.29 [5.66–10.62]*† |
| Mesenteric vascular resistance, mmHg·L ⁻¹ ·min ⁻¹ | | | | |
| Sham | 255 [197–370] | 304 [259–364] | 287 [189–359] | 264 [190–342] |
| Endotoxin shock | 286 [193–437] | 167 [109–260]*† | 269 [165–361] | 245 [180–333] |
| Left renal vascular resistance, dyn·s·cm ⁻⁵ | | | | |
| Sham | 535 [300–695] | 590 [450–740] | 600 [460–785] | 500 [460–710] |
| Endotoxin shock | 535 [325–805] | 315 [250–460]*† | 545 [340–610] | 635 [445–970] |
| Systemic O ₂ transport, mL·min ⁻¹ ·kg ⁻¹ | | | | |
| Sham | 17.4 [16.0–19.1] | 17.8 [15.9–22.3] | 18.1 [16.5–20.5] | 20.2 [15.7–23.4] |
| Endotoxin shock | 18.2 [14.6–22.5] | 12.3 [8.6–14.2]*† | 23.3 [11.3–30.8] | 20.0 [11.0–21.9] |
| Systemic O ₂ consumption, mL·min ⁻¹ ·kg ⁻¹ | | | | |
| Sham | 7.2 [6.3–8.2] | 7.4 [6.3–8.5] | 7.0 [6.2–8.1] | 7.1 [6.1–8.6] |
| Endotoxin shock | 7.1 [6.5–8.1] | 6.3 [5.6–6.6]*† | 7.3 [5.9–8.1] | 6.3 [5.9–8.2] |
| Systemic O ₂ extraction ratio | | | | |
| Sham | 0.40 [0.36–0.45] | 0.40 [0.33–0.47] | 0.41 [0.32–0.44] | 0.39 [0.32–0.45] |
| Endotoxin shock | 0.40 [0.29–0.48] | 0.54 [0.46–0.66]*† | 0.35 [0.27–0.52] | 0.36 [0.30–0.51] |
| Intestinal O ₂ transport, mL·min ⁻¹ ·100 g ⁻¹ | | | | |
| Sham | 5.1 [4.3–7.6] | 5.2 [4.0–7.6] | 5.4 [4.4–8.3] | 5.7 [4.6–9.5] |
| Endotoxin shock | 6.0 [4.0–8.7] | 3.4 [2.7–5.4]* | 4.5 [3.1–7.1] | 5.0 [3.2–7.6] |
| Intestinal O ₂ consumption, mL·min ⁻¹ ·100 g ⁻¹ | | | | |
| Sham | 2.1 [1.9–2.4] | 1.9 [1.7–2.1] | 2.2 [1.6–2.5] | 2.0 [1.4–2.6] |
| Endotoxin shock | 2.2 [1.6–2.9] | 2.2 [1.2–2.5] | 2.4 [1.6–3.1] | 2.7 [1.7–3.0] |
| Intestinal O ₂ extraction ratio | | | | |
| Sham | 0.42 [0.32–0.45] | 0.35 [0.30–0.44] | 0.33 [0.29–0.40] | 0.29 [0.25–0.34] |
| Endotoxin shock | 0.36 [0.30–0.48] | 0.52 [0.37–0.68]*† | 0.49 [0.38–0.72]*† | 0.51 [0.40–0.66]*† |

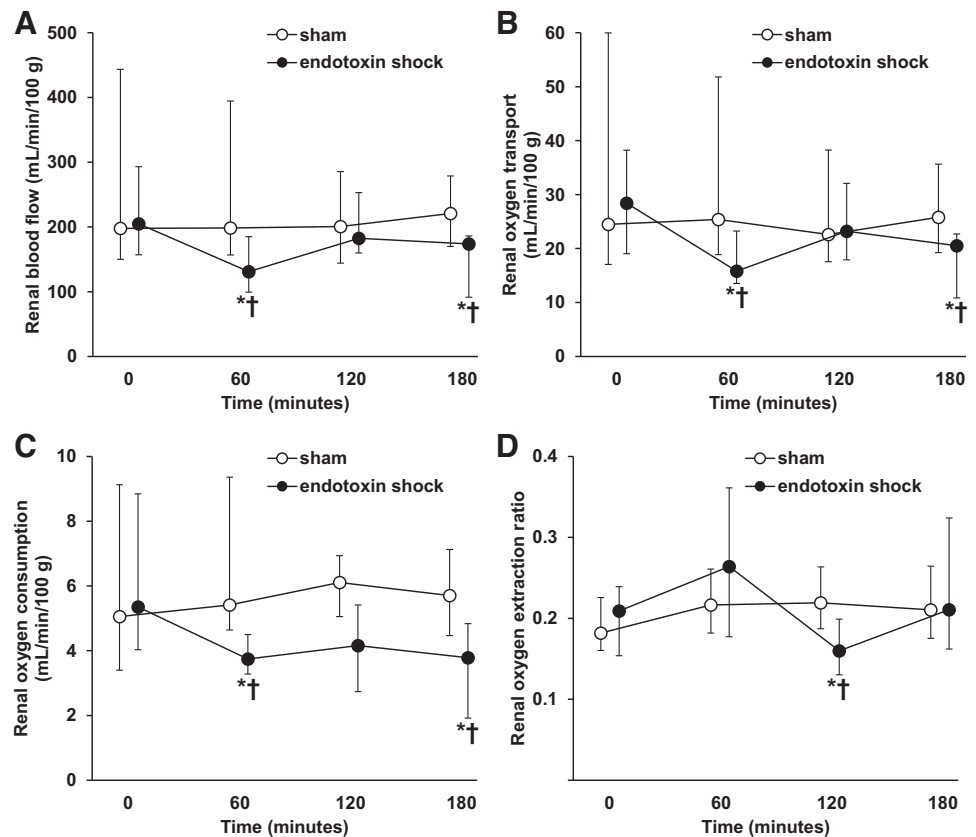
Data are shown as median [25–75 interquartile range]. * $P < 0.05$ vs. basal. † $P < 0.05$ vs. sham.

and creatinine clearance. The initial manifestations, including the fall in regional and microvascular flow, were the predictable consequence of the systemic cardiovascular compromise after endotoxin infusion. CI and RBF were severely decreased, and renal perfusion pressure reached values of ~30 mmHg, clearly exceeding the lower limit of autoregulation. The nor-

malization of systemic flow and the increase in MAP to 70 mmHg with fluids and norepinephrine only transiently improved renal perfusion, which eventually fell after 2 h of resuscitation.

Although the traditional standpoint is that septic AKI results from global hypoperfusion, several studies found normal or

Fig. 2. Behavior of renal hemodynamics and oxygen transport variables. Renal blood flow (A), oxygen transport (B), oxygen consumption (C), and oxygen extraction ratio (D). Data are shown as median [25–75 interquartile range]. † $P < 0.05$ vs. sham group. * $P < 0.05$ vs. baseline.



increased RBF, especially after the normalization of cardiac output by resuscitation (21, 30). Consistent with our results, a study performed in fluid-resuscitated rats with endotoxin shock showed a RBF of 70–85% of basal values, despite a 30% increase in CI (22). In pigs with endotoxin shock or fecal peritonitis, RBF also decreased, while CI normalized or even increased $>100\%$ (4, 23).

Notwithstanding the extremely low MAP and the fall of systemic and regional flows, endotoxin injection markedly decreased systemic, mesenteric, and renal vascular resistance. Abnormalities in vascular tone are indeed the key feature of septic shock, yet the reports about the response of renal vasculature in sepsis are contradictory (20). Challenging the traditional concept of increased renal vascular resistance in

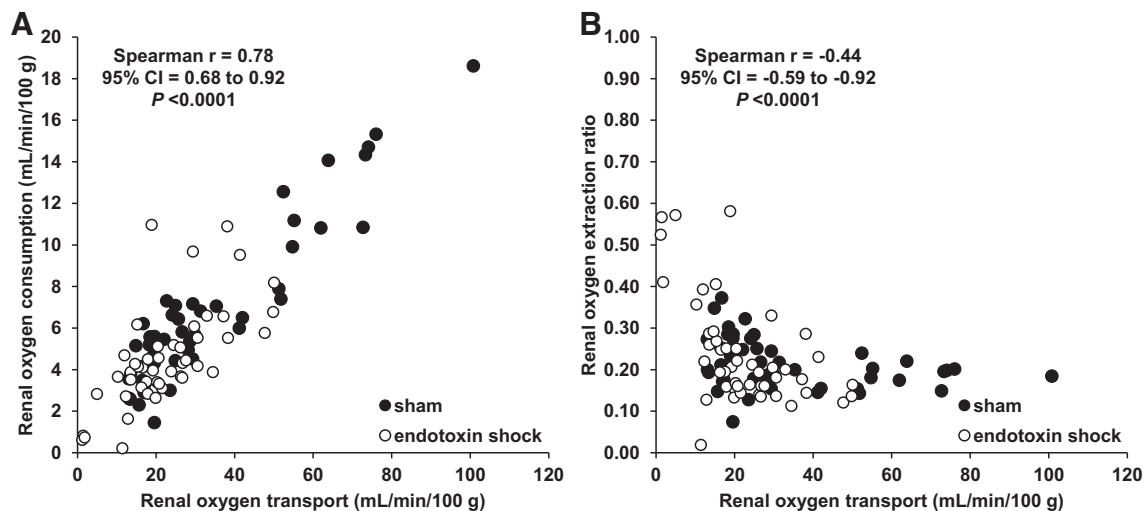


Fig. 3. Renal oxygen metabolism. Relationship between renal oxygen transport and consumption (A) and oxygen transport and extraction ratio (B). ●, Data from sham group; ○, data from endotoxin shock group. Spearman r displayed on the graphs are related to grouped values of both groups. A: renal oxygen transport and consumption were correlated in endotoxin shock [Spearman $r = 0.69$, 95% confidence interval (CI) = 0.50–0.82, $P < 0.0001$] and sham (Spearman $r = 0.86$, 95% CI = 0.76–0.92, $P < 0.0001$) group. B: renal oxygen transport and extraction ratio were correlated in endotoxin shock (Spearman $R = -0.51$, 95% CI = -0.70 to -0.26, $P < 0.0002$) and sham (Spearman $r = -0.38$, 95% CI = -0.61 to -0.10, $P < 0.001$) groups.

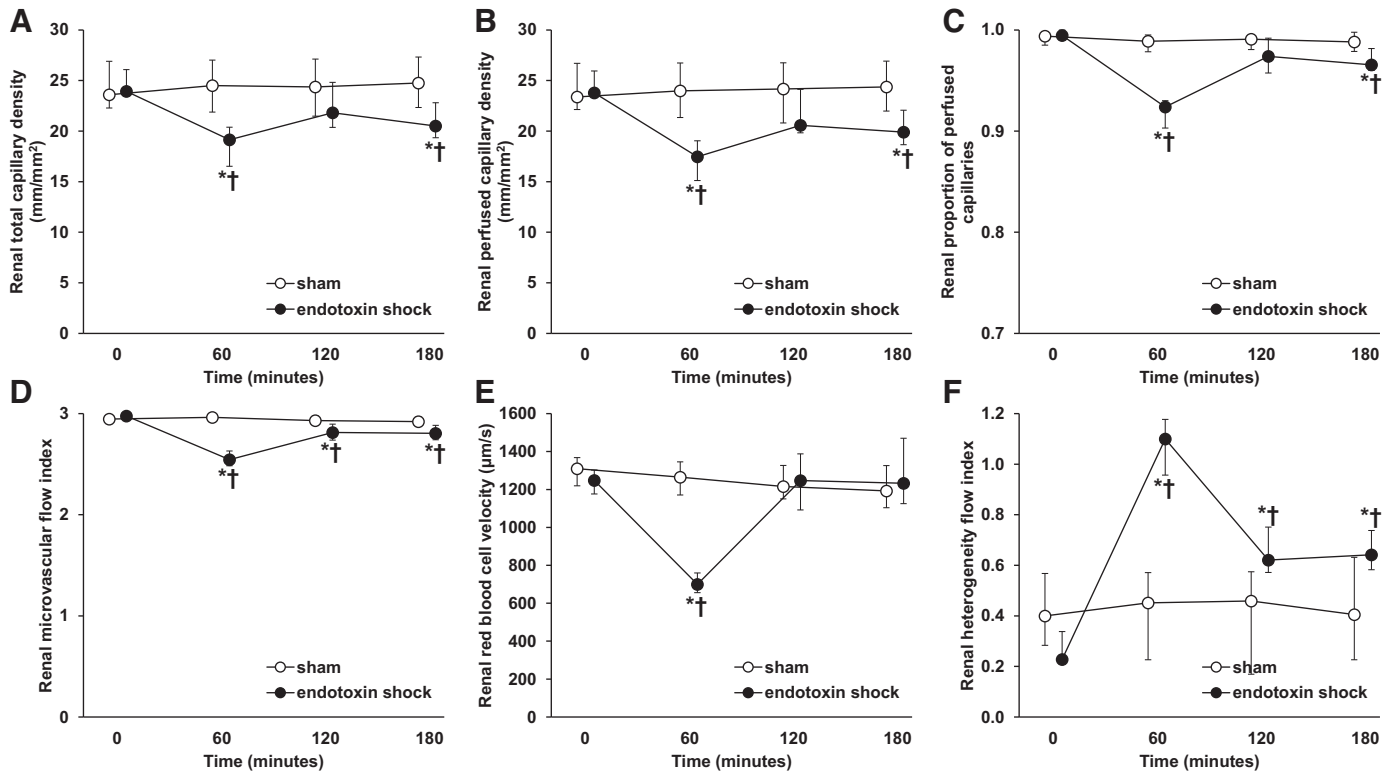


Fig. 4. Microcirculatory variables of the renal cortex in sham and endotoxin groups. *A*: total vascular density. *B*: perfused vascular density. *C*: proportion of perfused vessels. *D*: microvascular flow index. *E*: red blood cell (RBC) velocity. *F*: heterogeneity flow index. All the microcirculatory variables were compromised after 60 min of endotoxin shock. Resuscitation only normalized RBC velocity. Data are shown as median [25–75 interquartile range]. **P* < 0.05 vs. baseline. †*P* < 0.05 vs. sham group.

AKI, our findings of decreased resistance support the failure of autoregulation flow as an alternative mechanism; however, the increase in vascular tone generated by norepinephrine was unable to improve renal perfusion and function. Still, we cannot rule out that the vasopressor titration to higher MAP might have beneficial effects, as has already been described (5, 25). Future research should explore the effects of higher values of MAP as end points of resuscitation on renal microcirculation

and function. In another study, norepinephrine improved renal function only transiently, generating reductions in medullary but not in cortical perfusion and oxygenation (19).

The interpretation of renal $\dot{V}O_2$ and O_2ER behavior is not straightforward: we found decreases not only in shock but also during resuscitation, while others described a stable renal $\dot{V}O_2$ (24). The lack of O_2ER increase in response to reductions in DO_2 might be a consequence of microvascular shunting (15). In

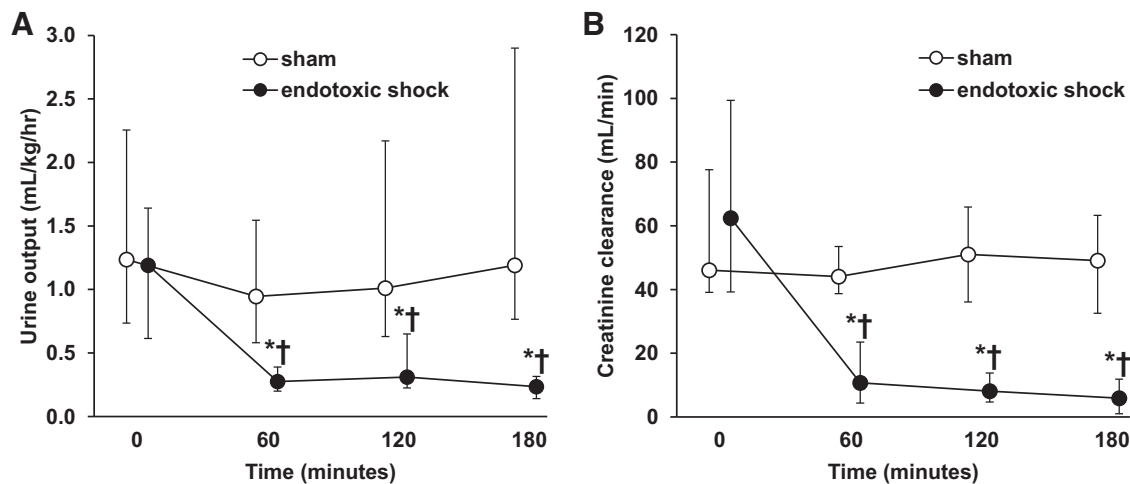


Fig. 5. Renal function. Behavior of urine output (*A*) and creatinine clearance (*B*) in sham and endotoxin groups. In the endotoxin shock group, both variables severely decreased after 60 min. Resuscitation failed to improve them. Data are shown as median [25–75 interquartile range]. **P* < 0.05 vs. baseline. †*P* < 0.05 vs. sham group.

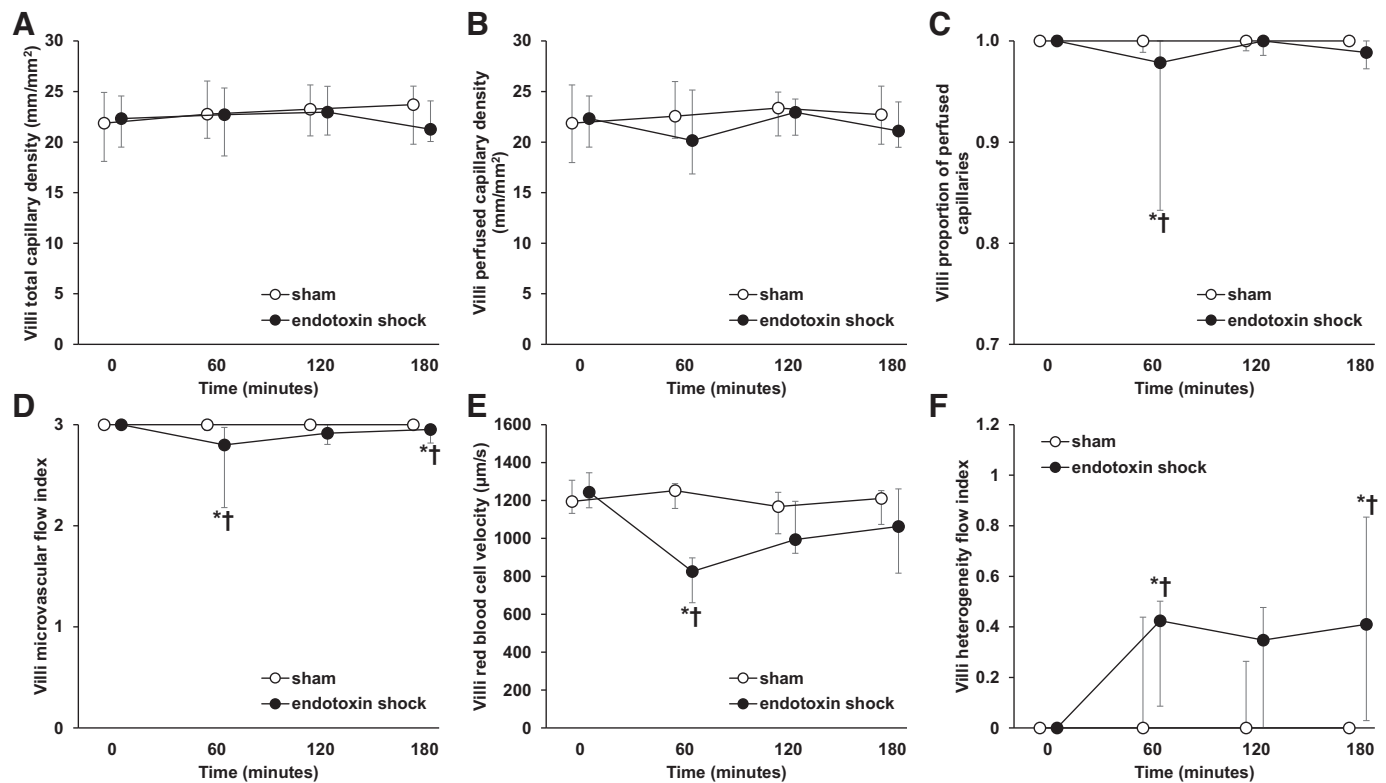


Fig. 6. Microcirculatory variables of the intestinal villi in sham and endotoxin groups. *A*: total vascular density. *B*: perfused vascular density. *C*: proportion of perfused vessels (PPV). *D*: microvascular flow index (MFI). *E*: red blood cell (RBC) velocity. *F*: heterogeneity flow index (HFI). Villi microcirculation showed minor but statistically significant decreases in the PPV and MFI during endotoxin shock. Resuscitation normalized PPV while MFI remained slightly but significantly decreased. RBC velocity decreased in endotoxin shock and normalized with resuscitation. HFI had manifest and persistent increases. Data are shown as median [25–75 interquartile range]. * $P < 0.05$ vs. baseline. † $P < 0.05$ vs. sham group.

the kidneys, however, the relationship between $\dot{V}O_2$ and DO_2 might reflect the normal behavior of the system. Falls in $\dot{V}O_2$ might not express development of anaerobic metabolism but suppression of nonessential functions, such as glomerular filtration rate and consequent tubular energy demand to avoid a dysoxic death (29). Accordingly, both the sham and endotoxin groups showed a significant correlation between $\dot{V}O_2$ and DO_2 . Another explanation for renal oxygen supply dependency might be a primary reduction in metabolic activity and oxidative metabolism induced by endotoxin (32). Thus reductions in regional and microvascular perfusion could have been homeostatic adjustments to match oxygen transport and needs.

The renal microcirculation probably plays a pivotal role in the pathophysiology of septic AKI (9, 26). Medullary ischemia and preservation of cortical perfusion have been considered the main features of the microvascular failure (3, 19, 24). Other investigators, however, have found cortical hypoperfusion (4, 13, 17, 22, 23, 34, 38). These conflicting results might be related to different models of septic shock and/or approaches to microcirculation. In our model, AKI was severe, unlike the mild or moderate compromise of renal function described in other studies (3, 5, 19, 24.). The use of laser Doppler flowmetry might explain the apparent preservation of cortical perfusion in those studies. This technique only provides a relative signal of RBC flow, comprising capillary, arterial, and venous blood flow, from an unknown tissue volume (33). Since no information on the absolute RBC velocity or velocity distribution is obtained, the technique cannot discriminate capillary stop-flow

or flow heterogeneity induced by sepsis. In contrast, SDF-videomicroscopy allows a thorough depiction of the density, perfusion, and heterogeneity characteristics of the microcirculation. In experimental septic shock, previous video micro-

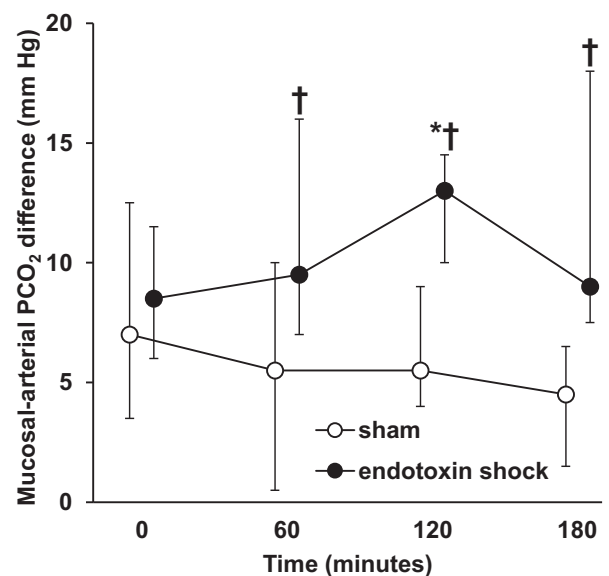


Fig. 7. Ileal mucosal minus arterial PCO_2 difference in sham and endotoxin groups. Data are shown as median [25–75 interquartile range]. * $P < 0.05$ vs. baseline. † $P < 0.05$ vs. sham group.

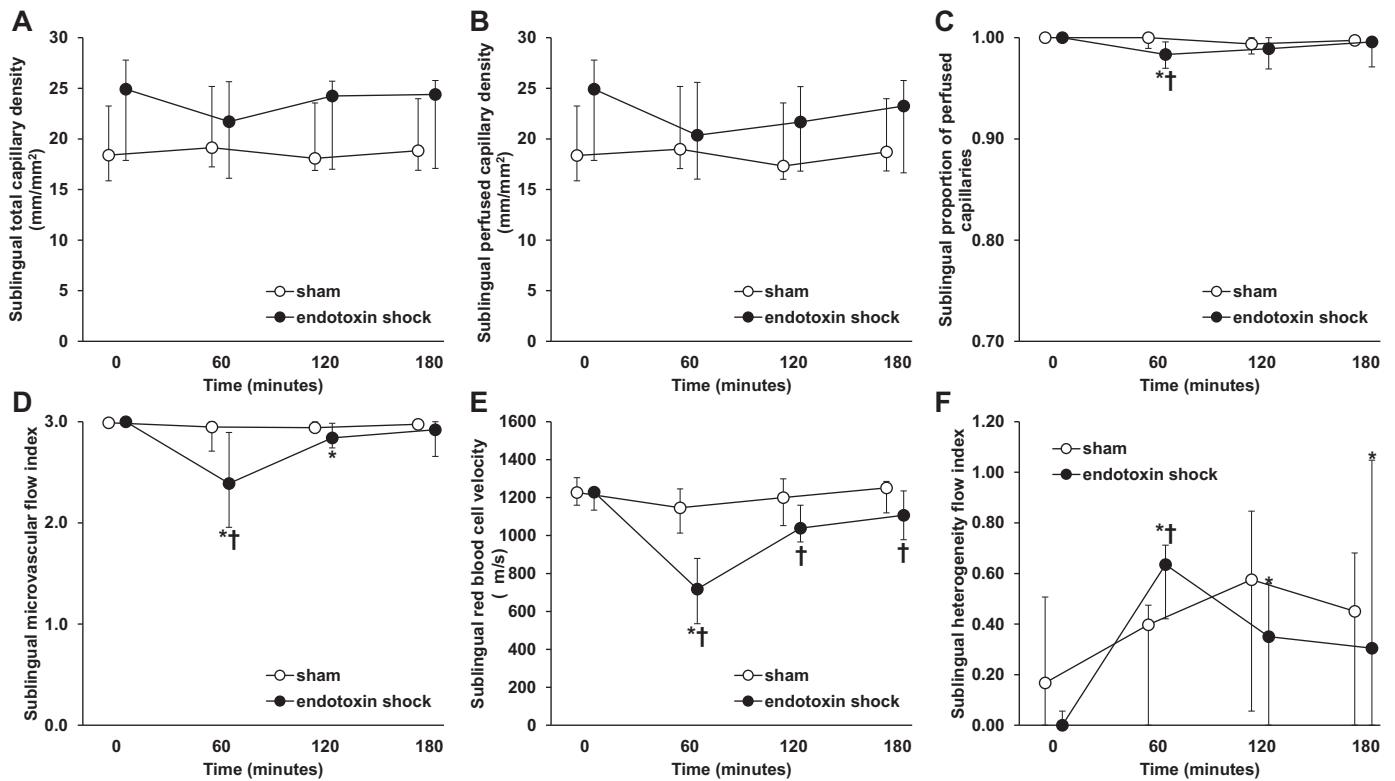


Fig. 8. Variables of sublingual microcirculation in sham and endotoxin group. *A*: total vascular density. *B*: perfused vascular density. *C*: proportion of perfused vessels (PPV). *D*: microvascular flow index (MFI). *E*: red blood cell (RBC) velocity. *F*: heterogeneity flow index (HFI). After 60 min of endotoxin shock, there were alterations in PPV, MFI, RBC velocity, and HFI. After resuscitation, only RBC velocity remained reduced compared with the sham group. Data are shown as median [25–75 interquartile range]. * $P < 0.05$ vs. baseline. † $P < 0.05$ vs. sham group.

scopic studies only gave a fragmentary description of cortical microcirculation (13, 34, 38). By means of a comprehensive analysis, our study showed that each one of the components of peritubular microcirculation was affected in shock, and that only RBC velocity was normalized by resuscitation. Recently, similar results were described using dynamic contrast-enhanced ultrasound (23).

Our study shows further evidence that microcirculation can be dissociated from systemic hemodynamics, and that the different microvascular beds might also be dissociated from each other. The gastrointestinal tract has been considered as the “canary of the body” (6); our results show that the kidney might be even more sensitive than the gut to endotoxin shock, in terms of both regional and tissue perfusion. On the contrary, other investigators reported a parallel involvement of sublingual and peritubular microcirculation beds (13, 23).

Another key question is whether the renal microvascular abnormalities described in this study only followed RBF reduction or expressed a primary microcirculatory failure. Microvascular dysfunction should be assessed considering the compromise of the different components of density, perfusion, and heterogeneity. Even though the fall in RBF after 3 h of shock and resuscitation was similar to that of cortical PVD (85 vs. 84% of basal values), there was a concurrent major increase in heterogeneity. Since heterogeneity of microvascular perfusion can deeply hamper tissue oxygen extraction (36), the extension of microvascular disturbances might exceed the simple fall in RBF. Derangements in microcirculatory perfusion might be even more meaningful in the first step of

endotoxin shock, since a large decrease in RBC velocity was also present. Yet, after 1 h of resuscitation, when RBF was transiently restored, some microcirculatory alterations persisted, suggesting these alterations were not a mere consequence of RBF reduction. The microcirculatory disorder might act as a kind of functional shunting, where signs of tissue dyoxia are evident despite apparent sufficient $\dot{V}O_2$ (16). Thus microcirculatory shunting might explain the inability to increase O_2ER and the consequent decrease in $\dot{V}O_2$.

The underlying mechanism for persistent renal microvascular dysfunction after restoration of systemic circulation might be the direct injury elicited by the septic insult (15). Cellular components at risk for endotoxin injury include the endothelium (14) and erythrocytes (1). Accordingly, animal models of sepsis showed a close association between peritubular capillary dysfunction and generation of reactive nitrogen species derived from inducible nitric oxide synthase (34, 38, 39). In addition, ischemia-reperfusion injury might play a role. Indeed, similar results were found in a pig model of aortic cross-clamping and reperfusion, in which intestinal and, particularly, renal microcirculatory oxygenation remained compromised after the restoration of systemic $\dot{V}O_2$ (31). The role of each mechanism should be explored in future studies by comparing the magnitude of microcirculatory dysfunction, in models of endotoxin administration and decreased blood flow produced by mechanical means.

Whichever the involved mechanism, our study showed that the improvement in MAP, CI, and $\dot{V}O_2$ failed to correct renal microcirculation and function. These findings suggest that

microcirculatory targets might be more adequate goals of resuscitation than systemic variables. An innovative and clinically feasible goal of resuscitation could be the correction of renal microcirculatory perfusion assessed by dynamic contrast-enhanced ultrasound (10, 23). Such a microcirculatory end point could be the subject of upcoming investigations.

Another mechanism that could contribute to AKI is the presence of intra-abdominal hypertension, a common complication of fluid resuscitation (37). This mechanism can be ruled out, since intra-abdominal pressure remained normal throughout the study.

Strengths of this study were the extensive assessment of systemic, regional, and microcirculatory hemodynamics, along with a comparison of different territories.

Our research has limitations. First, a short-term experiment might not reflect the more delayed responses described in other studies. Second, the evaluation of the renal microcirculation was restricted to cortical peritubular vessels. Third, allow the visualization of microcirculation, the kidney was decapsulated, which might have avoided a more severe derangement of renal function. Capsulotomy prevents an intrinsic renal compartment syndrome produced in experimental ischemia-reperfusion injury (11). Nevertheless, the brief period of resuscitation in our experiments probably precludes a role of decapsulation in ameliorating renal dysfunction. Last, we did not perform histological examinations, which precludes performing a correlation between structural damage and function. Nevertheless, gross tubular changes are usually absent in this experimental setting (18).

In conclusion, endotoxin shock induced severe AKI, which was initially associated with critical hypotension and systemic, regional, and microvascular hypoperfusion. Renal vascular resistance, however, showed manifest reductions as evidence of autoregulation failure. Increase in MAP to 70 mmHg and normalization of systemic hemodynamics by means of fluids and norepinephrine failed to improve RBF and cortical microcirculation. Nevertheless, the magnitude of these abnormalities might not be sufficient to explain the persistent and severe compromise of renal function. Other mechanisms such as inflammatory injury and compromise of medullary perfusion might also be involved.

ACKNOWLEDGEMENTS

This study was performed in Facultad de Ciencias Médicas, Universidad Nacional de La Plata, Cátedra de Farmacología Aplicada, 60 y 120, (1900) La Plata, Argentina.

DISCLOSURES

C. Ince has developed SDF imaging and is listed as the inventor on related patents commercialized by MicroVision Medical (MVM) under a license from the Academic Medical Center (AMC). He has been a consultant for MVM in the past but has not been involved with this company for more than 5 years and holds no shares in this company. Braedius Medical, a company owned by a relative of C. Ince, has developed and designed a hand-held microscope called CytoCam-IDF imaging. C. Ince has no financial relation with Braedius Medical of any sort, i.e., never owned shares or received consultancy or speaker fees from Braedius Medical. He hosts an internet site (<https://www.microcirculationacademy.org/>) that offers services (e.g., training, courses, and analysis) related to clinical microcirculation. None of the other authors has any conflicts of interest, financial or otherwise, to disclose.

AUTHOR CONTRIBUTIONS

G.F., V.S.K.E., J.F.C.E., M.G.B., H.S.C., B.L., L.G., C.I., and A.D. conceived and designed research; G.F., V.S.K.E., J.F.C.E., M.G.B., H.S.C., B.L., L.G., and A.D. performed experiments; G.F. and J.F.C.E. analyzed data; G.F., V.S.K.E., J.F.C.E., M.G.B., H.S.C., B.L., L.G., and A.D. interpreted results of experiments; G.F. and V.S.K.E. edited and revised manuscript; G.F., V.S.K.E., J.F.C.E., M.G.B., H.S.C., B.L., L.G., C.I., and A.D. approved final version of manuscript; A.D. prepared figures; A.D. drafted manuscript.

REFERENCES

- Bateman RM, Sharpe MD, Singer M, Ellis CG. The effect of sepsis on the erythrocyte. *Int J Mol Sci* 18: 1932, 2017. doi:10.3390/ijms18091932.
- Bouchard J, Acharya A, Cerda J, Maccariello ER, Madarasu RC, Tolwani AJ, Liang X, Fu P, Liu ZH, Mehta RL. A prospective international multicenter study of AKI in the intensive care unit. *Clin J Am Soc Nephrol* 10: 1324–1331, 2015. doi:10.2215/CJN.04360514.
- Calzavacca P, Evans RG, Bailey M, Bellomo R, May CN. Cortical and medullary tissue perfusion and oxygenation in experimental septic acute kidney injury. *Crit Care Med* 43: e431–e439, 2015. doi:10.1097/CCM.0000000000001198.
- Chvojka J, Sykora R, Krouzecky A, Radej J, Varnerova V, Karvunidis T, Hes O, Novak I, Radermacher P, Matejovic M. Renal haemodynamic, microcirculatory, metabolic and histopathological responses to peritonitis-induced septic shock in pigs. *Crit Care* 12: R164, 2008. doi:10.1186/cc7164.
- Corrêa TD, Vuda M, Takala J, Djafarzadeh S, Silva E, Jakob SM. Increasing mean arterial blood pressure in sepsis: effects on fluid balance, vasopressor load and renal function. *Crit Care* 17: R21, 2013. doi:10.1186/cc12495.
- Dantzker DR. The gastrointestinal tract. The canary of the body? *JAMA* 270: 1247–1248, 1993. doi:10.1001/jama.1993.03510100097040.
- Dobbe JG, Streekstra GJ, Atasever B, van Zijderveld R, Ince C. Measurement of functional microcirculatory geometry and velocity distributions using automated image analysis. *Med Biol Eng Comput* 46: 659–670, 2008. doi:10.1007/s11517-008-0349-4.
- Goedhart PT, Khalilzade M, Bezemer R, Merza J, Ince C. Sidestream dark field (SDF) imaging: a novel stroboscopic LED ring-based imaging modality for clinical assessment of the microcirculation. *Opt Express* 15: 15101–15114, 2007. doi:10.1364/OE.15.015101.
- Guerci P, Ergin B, Ince C. The macro- and microcirculation of the kidney. *Best Pract Res Clin Anaesthesiol* 31: 315–329, 2017. doi:10.1016/j.bpa.2017.10.002.
- Harrois A, Grillot N, Figueiredo S, Duranteau J. Acute kidney injury is associated with a decrease in cortical renal perfusion during septic shock. *Crit Care* 22: 161, 2018. doi:10.1186/s13054-018-2067-0.
- Herrler T, Tischer A, Meyer A, Feiler S, Guba M, Nowak S, Rentsch M, Bartenstein P, Hacker M, Jauch KW. The intrinsic renal compartment syndrome: new perspectives in kidney transplantation. *Transplantation* 89: 40–46, 2010. doi:10.1097/TP.0b013e3181c40aba.
- Hoste EA, Bagshaw SM, Bellomo R, Cely CM, Colman R, Cruz DN, Edipidis K, Forni LG, Gomersall CD, Govil D, Honoré PM, Joannes-Boyau O, Joannidis M, Korhonen AM, Lavrentieva A, Mehta RL, Palevsky P, Roessler E, Ronco C, Uchino S, Vazquez JA, Vidal Andrade E, Webb S, Kellum JA. Epidemiology of acute kidney injury in critically ill patients: the multinational AKI-EPI study. *Intensive Care Med* 41: 1411–1423, 2015. doi:10.1007/s00134-015-3934-7.
- Hua T, Wu X, Wang W, Li H, Bradley J, Peberdy MA, Ornato JP, Tang W. Micro- and macrocirculatory changes during sepsis and septic shock in a rat model. *Shock* 49: 591–595, 2018. doi:10.1097/SHK.0000000000000954.
- Ince C, Mayeux PR, Nguyen T, Gomez H, Kellum JA, Ospina-Tascón GA, Hernandez G, Murray P, De Backer D; ADQI XIV Workgroup. The endothelium in sepsis. *Shock* 45: 259–270, 2016. doi:10.1097/SHK.0000000000000473.
- Ince C, Mik EG. Microcirculatory and mitochondrial hypoxia in sepsis, shock, and resuscitation. *J Appl Physiol* (1985) 120: 226–235, 2016. doi:10.1152/jappphysiol.00298.2015.
- Ince C, Sinaasappel M. Microcirculatory oxygenation and shunting in sepsis and shock. *Crit Care Med* 27: 1369–1377, 1999. doi:10.1097/00003246-199907000-00031.
- Johannes T, Mik EG, Ince C. Nonresuscitated endotoxemia induces microcirculatory hypoxic areas in the renal cortex in the rat. *Shock* 31: 97–103, 2009. doi:10.1097/SHK.0b013e31817c02a5.

18. Kosaka J, Lankadeva YR, May CN, Bellomo R. Histopathology of septic acute kidney injury: a systematic review of experimental data. *Crit Care Med* 44: e897–e903, 2016. doi:10.1097/CCM.0000000000001735.
19. Lankadeva YR, Kosaka J, Evans RG, Bailey SR, Bellomo R, May CN. Intrarenal and urinary oxygenation during norepinephrine resuscitation in ovine septic acute kidney injury. *Kidney Int* 90: 100–108, 2016. doi:10.1016/j.kint.2016.02.017.
20. Langenberg C, Bellomo R, May CN, Egi M, Wan L, Morgera S. Renal vascular resistance in sepsis. *Nephron Physiol* 104: 1–11, 2006. doi:10.1159/000093275.
21. Langenberg C, Bellomo R, May C, Wan L, Egi M, Morgera S. Renal blood flow in sepsis. *Crit Care* 9: R363–R374, 2005. doi:10.1186/cc3540.
22. Legrand M, Bezemer R, Kandil A, Demirci C, Payen D, Ince C. The role of renal hypoperfusion in development of renal microcirculatory dysfunction in endotoxemic rats. *Intensive Care Med* 37: 1534–1542, 2011. doi:10.1007/s00134-011-2267-4.
23. Lima A, van Rooij T, Ergin B, Sorelli M, Ince Y, Specht PAC, Mik EG, Bocchi L, Kooiman K, de Jong N, Ince C. Dynamic contrast-enhanced ultrasound identifies microcirculatory alterations in sepsis-induced acute kidney injury. *Crit Care Med* 46: 1284–1292, 2018. doi:10.1097/CCM.0000000000003209.
24. Maiden MJ, Otto S, Brealey JK, Finnis ME, Chapman MJ, Kuchel TR, Nash CH, Edwards J, Bellomo R. Structure and function of the kidney in septic shock. A prospective controlled experimental study. *Am J Respir Crit Care Med* 194: 692–700, 2016. doi:10.1164/rccm.201511-2285OC.
25. Peng ZY, Critchley LA, Fok BS. The effects of increasing doses of noradrenaline on systemic and renal circulations in acute bacteraemic dogs. *Intensive Care Med* 31: 1558–1563, 2005. doi:10.1007/s00134-005-2741-y.
26. Post EH, Kellum JA, Bellomo R, Vincent JL. Renal perfusion in sepsis: from macro- to microcirculation. *Kidney Int* 91: 45–60, 2017. doi:10.1016/j.kint.2016.07.032.
27. Pozo MO, Kanoore Edul VS, Ince C, Dubin A. Comparison of different methods for the calculation of the microvascular flow index. *Crit Care Res Pract* 2012: 1–6, 2012. doi:10.1155/2012/102483.
28. Rhodes A, Evans LE, Alhazzani W, Levy MM, Antonelli M, Ferrer R, Kumar A, Sevransky JE, Sprung CL, Nunnally ME, Rochwerg B, Rubenfeld GD, Angus DC, Annane D, Beale RJ, Bellinhan GJ, Bernard GR, Chiche JD, Coopersmith C, De Backer DP, French CJ, Fujishima S, Gerlach H, Hidalgo JL, Hollenberg SM, Jones AE, Karnad DR, Kleinpell RM, Koh Y, Lisboa TC, Machado FR, Marini JJ, Marshall JC, Mazuski JE, McIntyre LA, McLean AS, Mehta S, Moreno RP, Myburgh J, Navalesi P, Nishida O, Osborn TM, Perner A, Plunkett CM, Ranieri M, Schorr CA, Seckel MA, Seymour CW, Shieh L, Shukri KA, Simpson SQ, Singer M, Thompson BT, Townsend SR, Van der Poll T, Vincent JL, Wiersinga WJ, Zimmerman JL, Dellinger RP. Surviving Sepsis Campaign: International Guidelines for Management of Sepsis and Septic Shock: 2016. *Crit Care Med* 45: 486–552, 2017. doi:10.1097/CCM.0000000000002255.
29. Schlichtig R, Kramer DJ, Boston JR, Pinsky MR. Renal O₂ consumption during progressive hemorrhage. *J Appl Physiol (1985)* 70: 1957–1962, 1991. doi:10.1152/jappl.1991.70.5.1957.
30. Schrier RW, Wang W. Acute renal failure and sepsis. *N Engl J Med* 351: 159–169, 2004. doi:10.1056/NEJMra032401.
31. Siegemund M, van Bommel J, Stegenga ME, Studer W, van Iterson M, Annaheim S, Mebazaa A, Ince C. Aortic cross-clamping and reperfusion in pigs reduces microvascular oxygenation by altered systemic and regional blood flow distribution. *Anesth Analg* 111: 345–353, 2010. doi:10.1213/ANE.0b013e3181e4255f.
32. Singer M. Metabolic failure. *Crit Care Med* 33, Suppl: S539–S542, 2005. doi:10.1097/01.CCM.0000186080.13402.96.
33. Smits GJ, Roman RJ, Lombard JH. Evaluation of laser-Doppler flowmetry as a measure of tissue blood flow. *J Appl Physiol (1985)* 61: 666–672, 1986. doi:10.1152/jappl.1986.61.2.666.
34. Tiwari MM, Brock RW, Megyesi JK, Kaushal GP, Mayeux PR. Disruption of renal peritubular blood flow in lipopolysaccharide-induced renal failure: role of nitric oxide and caspases. *Am J Physiol Renal Physiol* 289: F1324–F1332, 2005. doi:10.1152/ajprenal.00124.2005.
35. Trzeciak S, Dellinger RP, Parrillo JE, Guglielmi M, Bajaj J, Abate NL, Arnold RC, Colilla S, Zanotti S, Hollenberg SM; Microcirculatory Alterations in Resuscitation and Shock Investigators. Early microcirculatory perfusion derangements in patients with severe sepsis and septic shock: relationship to hemodynamics, oxygen transport, and survival. *Ann Emerg Med* 49: 88–98, 2007. doi:10.1016/j.annemergmed.2006.08.021.
36. Walley KR. Heterogeneity of oxygen delivery impairs oxygen extraction by peripheral tissues: theory. *J Appl Physiol (1985)* 81: 885–894, 1996. doi:10.1152/jappl.1996.81.2.885.
37. Wauters J, Claus P, Brosens N, McLaughlin M, Malbrain M, Wilmer A. Pathophysiology of renal hemodynamics and renal cortical microcirculation in a porcine model of elevated intra-abdominal pressure. *J Trauma* 66: 713–719, 2009. doi:10.1097/TA.0b013e31817c5594.
38. Wu L, Gokden N, Mayeux PR. Evidence for the role of reactive nitrogen species in polymicrobial sepsis-induced renal peritubular capillary dysfunction and tubular injury. *J Am Soc Nephrol* 18: 1807–1815, 2007. doi:10.1681/ASN.2006121402.
39. Wu L, Mayeux PR. Effects of the inducible nitric-oxide synthase inhibitor L-N(6)-(1-iminoethyl)-lysine on microcirculation and reactive nitrogen species generation in the kidney following lipopolysaccharide administration in mice. *J Pharmacol Exp Ther* 320: 1061–1067, 2007. doi:10.1124/jpet.106.117184.